Scientific Reports

https://doi.org/10.1038/s41598-026-38694-2

Article in Press

High-capacity and secure inter-satellite optical wireless communication using 2D DPS-OCDMA

Received: 20 September 2025

Accepted: 30 January 2026

Published online: 09 February 2026

Cite this article as: Armghan A., Abd El-Mottaleb S.A., Aldkeelalah S.S. *et al.* High-capacity and secure inter-satellite optical wireless communication using 2D DPS-OCDMA. *Sci Rep* (2026). https://doi.org/10.1038/s41598-026-38694-2

Ammar Armghan, Somia A. Abd El-Mottaleb, Sultan S. Aldkeelalah, Slim Chaoui, Ahmed Emara & Mehtab Singh

High-Capacity and Secure Inter-Satellite Optical Wireless Communication Using 2D DPS-OCDMA

Ammar Armghan[1*], Somia A. Abd El-Mottaleb[2], Sultan S. Aldkeelalah[3], Slim Chaoui[4], Ahmed Emara[5,6], Mehtab Singh[7]

[1]Department of Electrical Engineering, College of Engineering, Jouf University, Sakaka 72388, Saudi Arabia (aarmghan@ju.edu.sa)

[2] Department of Mechatronics Engineering, Alexandria Higher Institute of Engineering and Technology, Alexandria, Egypt (somaya8839@gmail.com)

[3]Department of Electrical Engineering, College of Engineering, Jouf University, Sakaka 72388, Saudi Arabia (saldkeelalah@ju.edu.sa)

[4]Department of Computer Engineering and Networks, College of Computer and Information Sciences, Jouf University, Sakaka 72388, Saudi Arabia (schaoui@ju.edu.sa)

[5]Electrical Engineering Department, University of Business and Technology, Ar Rawdah, Jeddah 23435, Saudi Arabia (a.emara@ubt.edu.sa)

[6]Department of Engineering Mathematics and Physics, Faculty of Engineering, Alexandria University, Alexandria, Egypt

[7] Department of Electronics and Communication Engineering, University Institute of Engineering, Chandigarh University, Mohali, Punjab, India (mehtab91singh@gmail.com)

*Corresponding author email ID: aarmghan@ju.edu.sa

Abstract: Inter-satellite optical wireless communication (IsOWC) has emerged as a promising technology for high-capacity and secure links in next-generation satellite networks. The overall system efficiency, however, is highly dependent on several design factors, including the receiver aperture size, pointing error, optical efficiency, and additional propagation losses, which must be carefully addressed to ensure reliable operation over long inter-satellite distances This paper proposes an enhanced IsOWC model that employs two-dimensional optical code division multiple access

(2D-OCDMA) based on diagonal permutation shift (DPS) codes to enhance link capacity while maintaining secure transmission. The proposed system is assessed under diverse channel scenarios by altering the inter-satellite link (ISL), the diameter of the receiving aperture, pointing inaccuracies, optical transmission efficiency. System performance is evaluated using metrics including bit error rate (BER), Q-factor, and visual inspection. The results demonstrate that the adoption of 2D-OCDMA significantly improves transmission quality, achieving reliable communication over ranges up to 16,000 km. Furthermore, using 2D DPS code provides inherent security, since data can only be decoded by receivers equipped with the proper code sequence. Additionally, the proposed system supports an overall data rate of 120 Gbps with BER values well below the forward error correction (FEC) threshold (3.8×10^{-3}) under realistic conditions.

Keywords: Intersatellite optical wireless communication (IsOWC) system; 2D diagonal permutation shift code (2D DPS), pointing error, receiver aperture diameter, optical efficiencies, bit error rate (BER).

1. Introduction

The next generation of mobile satellite communication systems is anticipated to provide widespread, adaptable, and high-quality multimedia connectivity to users, regardless of their location or when they access the service [1]. A central vision of such systems is enabling seamless communication between any two points across the globe. One practical approach to realize this objective is through the establishment of interconnected satellite constellations in conjunction with terrestrial gateway stations. When communicating parties are on opposite sides of the Earth, data is relayed sequentially between satellites via ISLs until it reaches its destination in ground station. ISLs are therefore crucial for achieving seamless global communication coverage. To support such functionality, satellites must be equipped with advanced high-speed processing and switching capabilities.

Traditional inter-satellite communication has predominantly employed radio frequency (RF) links. However, RF systems are inherently constrained by limited bandwidth and the necessity of mitigating interference, which restricts their ability to achieve very high transmission speeds [2]. Optical inter-satellite communication known as intersatellite-optical-wireless-communication (IsOWC), on the other hand, overcomes many of these drawbacks. Optical carrier frequencies for ISL have been internationally standardized within the ranges of approximately 200 THz (1550 nm) and 350 THz (850 nm) [3]. Unlike conventional RF bands, these optical transmission windows are globally unlicensed and do not generate

interference with satellite or terrestrial RF systems. Building on this advantage, optical links exploit the extremely high carrier frequencies and wide spectral bandwidth to deliver high-speed, high-capacity data transfer. The use of optical wavelengths also ensures immunity to radio interference while enabling compact and lightweight terminals. Furthermore, the short wavelengths provide high antenna gain and narrow beam divergence with relatively small apertures, leading to reduced payload weight and, consequently, lower launch costs with enhanced overall system efficiency [4].

In IsOWC systems, data is exchanged between satellites through optically modulated carriers that propagate in free space or vacuum. The use of narrow laser beams significantly reduces transmission losses compared to conventional microwave or RF systems. The operating principle is analogous to that of optical fiber communication, except that free space serves as the propagation medium. Reliable operation requires a clear line-of-sight (LoS) between terminals, which is maintained through accurate acquisition, pointing, and tracking mechanisms [6].

Inter-satellite optical communication has been the subject of significant experimental investigations led by major international space agencies, such as the European Space Agency (ESA), the Japan Aerospace Exploration Agency (JAXA), the German Aerospace Center (DLR), and the National Aeronautics and Space Administration (NASA) [5].

In 2001, a significant achievement was recorded when a 50 Mbps IsOWC link was established between the geostationary orbit (GEO)-based ARTEMIS satellite, and the low Earth orbit (LEO)-based SPOT-4 satellite [7].

In 2014, the European Data Relay Satellite (EDRS) program marked a major step forward in IsOWC. During November of that year, a data link was successfully demonstrated between Sentinel-1A, operating in LEO, and Alphasat, positioned in GEO. A series of follow-up experiments were then carried out the following month. These December trials not only validated the earlier results but also revealed that the link performance went beyond what the system had originally been designed to achieve [8]. Recently in 2024, JAXA achieved the world's fastest IsOWC at a speed of 1.8 Gbps between the Laser Utilizing Communication System (LUCAS) and the Advanced Land Observing Satellite-4 “DAICHI-4” (ALOS-4) [9].

However, the performance of IsOWC links is constrained by several critical factors that must be carefully managed. Maintaining precise alignment and pointing accuracy between satellites is fundamental, as even small deviations can destabilize the optical link. Transmission efficiency is

further influenced by optical beam divergence and free-space path loss, which become more pronounced over long inter-satellite distances. Additionally, mechanical and thermal-induced satellite vibrations, together with platform jitter, can compromise the LoS requirement, leading to intermittent signal loss. Beyond physical link constraints, effective latency control and precise time synchronization are essential to guarantee seamless and reliable data exchange across the network, particularly in high-speed communication scenarios [10].

To enhance the transmission capacity of IsOWC systems, various multiplexing strategies have been employed, including Wavelength-Division-Multiplexing (WDM) [11], Orthogonal-Frequency-Division-Multiplexing (OFDM) [6], Polarization Division Multiplexing (PDM) [11], Orbital Angular Momentum (OAM) multiplexing [12], and Optical Code Division Multiple Access (OCDMA) (Al Hammadi and Islam, 2020; Abd El-Mottaleb et al., 2023).

In this work, we use two-dimension (2D) OCDMA that utilized diagonal permutation shift code for enhancing the IsOWC capacity. OCDMA is a multiplexing approach designed to enhance transmission capacity by allowing multiple users to share a single wavelength and time slot without requiring strict wavelength control or time synchronization, thanks to code-domain asynchrony. In this technique, each channel is assigned a distinct code represented by a sequence of “1” and “0” bits, where each “1” corresponds to the presence of light at a specific wavelength. OCDMA can be realized using one-dimensional (1D) or (2D) codes. Common 1D coding schemes include Modified Double Weight (MDW), Permutation Vector (PV), Fixed Right Shift (FRS), and Diagonal Permutation Shift (DPS), although the code length (N) limits the number of users and, consequently, the multiplexing capacity. To overcome these constraints, 2D codes combine two parameters including spectral, spatial, temporal, or polarization, providing higher user capacity without increasing code length, improving security, and reducing multi-user interference.

While multiplexing techniques such as WDM, OFDM, PDM, OAM, and SAC-OCDMA have enhanced IsOWC capacity by adding spectral channels, subcarriers, modes, or polarizations, they do not employ a 2D DPS code structure jointly in the spectral–polarization domain at the code level. In contrast, the proposed 2D DPS-OCDMA uses a DPS sequence duplicated over two orthogonal polarization states, effectively doubling the DPS user set for a fixed code length (C=12) and fixed number of wavelengths (four), while preserving low cross-correlation and MAI suppression via SPD/S-decoder detection. This differs from PDM or WDM applied atop existing codes, as polarization is embedded in the 2D code design, enabling high

spectral efficiency per wavelength, intrinsic physical-layer security through code secrecy, and robustness against MAI without tight user synchronization.

1.1 Contribution

As DPS code shows good performance in free space optics system and underwater optical wireless communication system, in this paper, we use it but 2D OCDMA for the first time in IsOWC system for enhancing transmission capacity between satellites and provide secure data transmission. The main contributions of this work can be summarized as follows:

- Novel IsOWC architecture: We propose, for the first time, an IsOWC system based on 2D DPS codes in an OCDMA framework. The use of 2D DPS codes enables both enhanced transmission capacity (120 Gbps) and secure data transmission, as only receivers with the correct code can successfully recover the signal.
- Comprehensive system performance analysis: We investigate the performance of the proposed system under a wide range of practical conditions, including:
  - Inter-satellite link distances between 12,000 km and 16,000 km,
  - Receiver aperture diameters of 10–20 cm,
  - Receiver pointing errors between 1–1.5 μrad, and
  - Optical efficiency values in the range of 0.7–0.9,
- Performance evaluation metrics: We evaluate the system performance using BER analysis, Q-factors and eye diagram characterization, providing detailed insights into the impact of system parameters on link reliability, transmission quality, and signal integrity.

The remainder of this paper is structured as follows. Section 2 provides a comprehensive review of related studies on IsOWC systems, highlighting their limitations and motivating the need for our proposed approach. Section 3 details the construction of the 2D DPS code, including its design principles and suitability for high-capacity optical communication. Section 4 presents the architecture of the proposed IsOWC system, outlining the key components and operational assumptions. Section 5 reports and discusses the simulation results, analyzing system performance under varying parameters. Finally, Section 6 concludes the paper by summarizing the key findings and outlining potential directions for future research.

2. Related Work

A considerable number of studies have investigated the design, performance, and applications of IsOWC. Authors in [13] studied the performance of IsOWC with dense WDM (DWDM) and subcarrier multiplexing significantly enhances system capacity. Implementations at wavelengths of 850, 1064, and 1550 nm show improved Q-factor and reduced bit error rate (BER), with achievable data rates scaling with the number of multiplexed channels. These findings confirm that multiplexing-based IsOWC systems offer superior performance compared to single-channel PSK systems while maintaining compatibility with existing optical infrastructure. However, the effect of transmission distance, pointing error, and receiver aperture diameter were not considered in that study. In [14], a high- IsOWC link based on mode division multiplexing (MDM) was modeled and analyzed. Simulation results indicated successful transmission of 2 × 40 Gbps data over a 6000 km link with satisfactory performance metrics, achieving a Q-factor above 6 dB and a BER not exceeding 10^{-9}. The study further examined the influence of pointing errors, showing that even with a 2 μrad misalignment, reliable transmission of 2 × 40 Gbps was maintained over a reduced distance of 4000 km. In [15], an IsOWC system was designed to establish a 1000 km link between two satellites at a data rate of 2.5 Gbps, both with and without the use of a square root module (SM). Simulation outcomes demonstrated that incorporating the SM module improved the signal-to-noise ratio (SNR) and maintained an acceptable BER over the 1000 km inter-satellite link. Furthermore, it was observed that less transmitted optical power was required to deliver 2.5 Gbps externally modulated data at an operating wavelength of 1550 nm when the SM module was utilized. However, that study did not evaluate the impact of pointing error which is one of the major challenges that effect the IsOWC system. In [16], the transmission of 10 Gbps data over a 4000 km inter-satellite optical wireless communication link was investigated using an OFDM scheme. The study also compared the performance of 4-quadrature amplitude modulation (4-QAM) and 4-phase shift keying (4-PSK) encoding techniques. System evaluation was carried out in terms of SNR, total received power, radio-frequency spectrum, and constellation diagrams, demonstrating the feasibility of OFDM for long-haul IsOWC links. In [3], researchers developed an IsOWC system to support connectivity between GEO and LEO satellites across a 45,000 km distance at a data rate of 2 Gbps. To enhance link reliability, different multiplexing and diversity schemes were analyzed with the objective of achieving a Q-factor improvement and a BER threshold of 10^{-6}. At the operating wavelength of 850 nm, the received optical signal power was reported as 4.3825. The study further examined the role of multiple-input multiple-output (MIMO), which produced a Q-

factor of 4.1803. On the other hand, WDM demonstrated clear performance gains, elevating the Q-factor to a peak value of 4.74494. However, this investigation did not account for additional impairments such as pointing errors, platform vibrations, or other potential loss factors, which may significantly affect real-world IsOWC link performance. Authors in [12] investigated the integration of orbital angular momentum (OAM) multiplexing with IsOWC links to enable high-speed data transmission for space applications. In their work, four distinct OAM beams were utilized to transmit independent 20 Gbps binary data streams over an OWC channel between two satellites, achieving an aggregate data rate of 80 Gbps. System performance was assessed in terms of link range, misalignment pointing errors, additional losses from solar radiation, and--++++ laser transmission power through numerical simulations. The results demonstrated reliable 80 Gbps transmission over a 10,000 km ISL at 30 dBm laser power, sustaining a log(BER) ≤ –5 under 1.6 μrad pointing error and 5 dB additional losses. Moreover, reducing the pointing error to 1 μrad extended the achievable range to 12,000 km while maintaining log(BER) ≤ –5. Nevertheless, the study did not address physical-layer security aspects, leaving the system potentially vulnerable to interception and eavesdropping in practical inter-satellite communication scenarios. Recently, Zhu et al. [17] investigated the average BER performance of inter-satellite optical communication (ISOC) systems under the combined influence of orbital perturbations and platform vibrations. Their work introduced probability density functions for perturbation-induced radial displacement and pointing errors and derived a closed-form expression for system BER using the Meijer G-function. This pioneering analysis highlighted the crucial role of orbital radius and relative satellite states in determining ISOC link robustness. Furthermore, Xu et al. [18] extended this investigation to satellite-to-ground optical communication (SGOC) systems, integrating the effects of orbital deviations and atmospheric turbulence. Their model combined gamma-gamma turbulence fading with pointing errors derived from orbital motion, yielding closed-form BER expressions and simulation validations. These results elucidated the impact of orbital altitude, initial relative velocity, and antenna elevation on link performance.

While the above-mentioned studies have advanced the development of inter-satellite OWC systems, many of them do not fully account for critical factors such as pointing errors, additional transmission losses, achievable link distances, and communication security. The novelty of the present work lies in addressing these limitations by incorporating all these aspects into the system design. Specifically, this study introduces an OCDMA-based 2D DPS code scheme, which not only mitigates the impact of

pointing errors and link losses but also enhances system security, thereby enabling reliable and secure high-capacity inter-satellite communication.

While the above studies advance IsOWC multiplexing, they lack a 2D DPS-OCDMA scheme tailored for inter-satellite links: prior OCDMA uses other codes (e.g., SAC, MDW) not exploiting DPS's unity cross-correlation in 2D spectro-polarization, and often omit joint analysis of pointing error, aperture limits, and losses over long ranges. Our work addresses these gaps by introducing 2D DPS-OCDMA, achieving 120 Gbps with BER below FEC threshold under these constraints.

3. Construction of 2D DPS-OCDMA Code

The proposed 2D DPS construction for OCDMA-based IsOWC systems extends the conventional 1D DPS code into a spectral–polarization domain to enhance user capacity. The first three N rows of the 1D DPS matrix, constructed as described in [19], are used as input to the 2D DPS procedure which are as follows:

$$\text{1D DPS matrix} = \begin{bmatrix}0110\\1011\\1102\end{bmatrix}^{T} \begin{bmatrix}100 & 010 & 010 & 100\\010 & 100 & 010 & 010\\010 & 010 & 100 & 001\end{bmatrix} \tag{1}$$

Each DPS row is duplicated across two polarization states, horizontal (H) and vertical (V), with all chips in a given row transmitted using the same polarization to simplify hardware implementation. Spectral channels correspond directly to the elements of each DPS row, and each element is mapped to a 3-bit code ($0 \rightarrow 100$, $1 \rightarrow 010$, $2 \rightarrow 001$) for OCDMA transmission. This approach effectively doubles the user capacity by exploiting the polarization dimension while maintaining the orthogonality provided by the spectral domain. The detailed steps of the 2D DPS construction are summarized in Algorithm 1.

Algorithm 1 Construction of 2D DPS Code (Spectral × Polarization) for OCDMA-based IsOWC System

Input: w (DPS code weight), K (number of DPS channels = w^2), C (DPS code length = $K + w$), N_users (number of 1D DPS users to use), Spectral channels (λ_1, λ_2, λ_3, λ_4), Polarization (H, V), DPS_1D (first N_users rows of 1D DPS matrix)
Output: 2D DPS code sequences (spectral × polarization)
Procedure: 2D DPS Code Construction

```
if w < 2 or w is not odd then
    Print ("Invalid DPS code weight. Algorithm terminated.")
    End procedure
Initialize DPS_2D_sequences as empty list
for user_index = 1to N_users do
    DPS_row = DPS_1D[user_index]
```

```
    for each pol in Polarizations do // Duplicate row for H and V
      Initialize empty code_sequence
      for col_index = 1 to length(DPS_row) do
        element = DPS_row[col_index]
        spectral = SpectralChannels[col_index]
        if element == 0 then chip_code = "100"
        else if element == 1 then chip_code = "010"
        else if element == 2 then chip_code = "001"
        Append (chip_code, spectral, pol) to code_sequence
      end for
      Append code_sequence to DPS_2D_sequences
    end for
  end for
  Return DPS_2D_sequences
```

Table 1 summarizes the 2D DPS code assignment for the first six users, showing how the first three DPS users are transmitted in both horizontal (H) and vertical (V) polarizations to effectively double the user capacity.

Table 1 2D DPS code assignment for first six users with dual polarization (H/V) and corresponding 3-bit OCDMA codes.

Channel	DPS row from 1D DPS matrix	Spectral channel	Polarization	3-bit code sequence
1H	[0110]	λ_1	H	100
		λ_2		010
		λ_3		010
		λ_4		100
2H	[1011]	λ_1	H	010
		λ_2		100
		λ_3		010
		λ_4		010
3H	[1102]	λ_1	H	010
		λ_2		010
		λ_3		100
		λ_4		001
1V	[0110]	λ_1	V	100
		λ_2		010
		λ_3		010
		λ_4		100
2V	[1011]	λ_1	V	010

		λ_2		100
		λ_3		010
		λ_4		010
3V	[1102]	λ_1	V	010
		λ_2		010
		λ_3		100
		λ_4		001

The channels with their corresponding code sequences and wavelengths are given in Table 2.

Table 2 Channels with corresponding code sequences and wavelengths.

Channel	Code sequence	Wavelength (nm)
1 (1H)	100 010 010 100	850, 853.2, 855.6, and 856.6
2 (2H)	010 100 010 010	850.8, 852.4, 855.6, and 857.4
3 (3H)	010 010 100 001	850.8, 853.2, 854.8, and 858.8
4 (1V)	100 010 010 100	850, 853.2, 855.6, and 856.6
5 (2V)	010 100 010 010	850.8, 852.4, 855.6, and 857.4
6 (3V)	010 010 100 001	850.8, 853.2, 854.8, and 858.8

4. Design of Proposed IsOWC based on using 2D DPS Code

In this work, we supposed data transmission between two satellites using optical carriers as illustrated in Fig. 1.

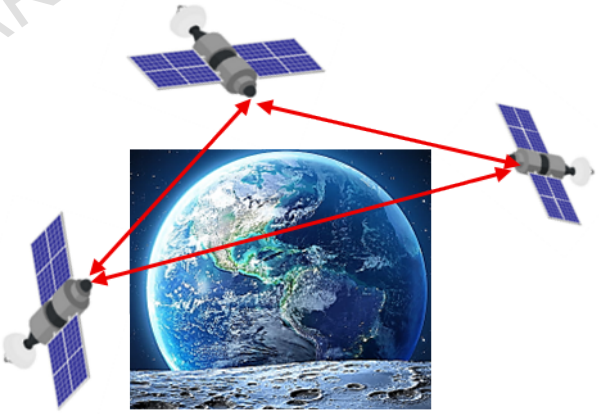

Figure 1 Data transmission between satellites.

Figure 2 shows the design of the proposed 1. IsOWC based on using 2D DPS code. It consists of transmitter, channel, and receiver.

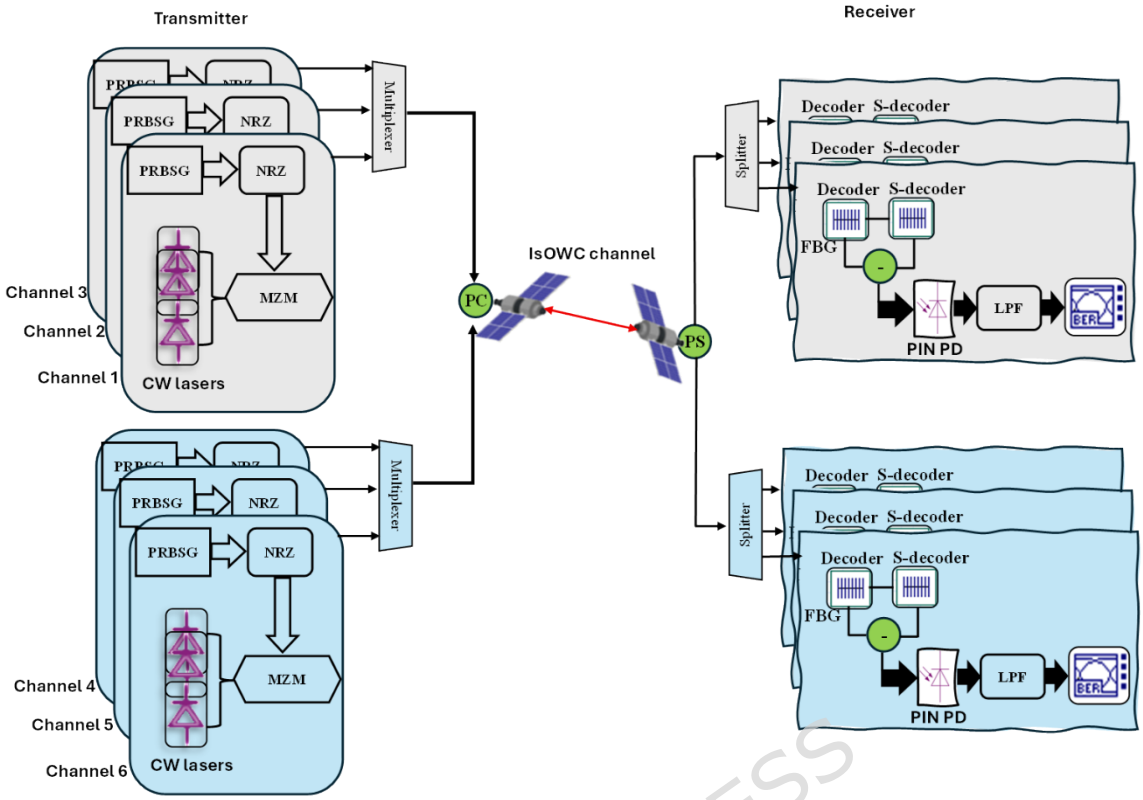

Figure 2 Design of the proposed IsOWC based on using 2D DPS code.

4.1 Transmitter

At the transmitter of the first satellite, a pseudo–random bit sequence (PRBS) generator produces binary symbols at R_b = 20 Gbps per channel. The binary stream is On-Off Keying (OOK) Non-Return-To-Zero (NRZ) line–encoded to form the baseband envelope that expressed as:

$$E_{NRZ}(t) = \sum_{i=0}^{M-1} a_i \Pi\left(\frac{t - iT_b}{T_b}\right) \quad (2)$$

where $a_i \in \{0, 1\}$ denotes the i^{th} bit amplitude symbol, $\Pi(\bullet)$ is the unit rectangular pulse of duration T_b, where $T_b = 1/R_b$.

As for optical carrier per each channel, continuous wave (CW) lasers are used which have wavelengths as given in Table 2. For each channel, the complex optical field of the i^{th} CW source is expressed as:

$$E_{c,i}(t) = E_{A,i} e^{j(2\pi f_{c,i} t + \theta_{c,i})} e_{c,i} \quad (3)$$

where $E_{A,i}$ is the carrier amplitude, $f_{c,i}$ refers to the optical frequency, and $\theta_{c,i}$ denotes the phase shift angle which is set to 0°. The parameter $e_{c,i}$ depicts the unit polarization vector (e.g., $\hat{x}$ for H and $\hat{y}$ for V) of the CW which equal to $e_x + e_y e^{j\frac{\pi}{2}}$.

As four wavelengths are assigned per channel, so, the combined optical signal is given as

$$E_c(t) = \sum_{i=1}^{4} E_{A,i} e^{j(2\pi f_{c,i} t + \theta_{c,i})} e_{c,i} \quad (4)$$

The electric signal that carries the data is then modulated on optical combined signal through using a Mach-Zehnder modulator (MZM). The output optical signal from the MZM is expressed as

$$E_{MZM}(t) = \cos\left(\frac{\pi V(t)}{2V_\pi} + \varphi_b\right) \sum_{i=1}^{4} E_{A,i} e^{j(2\pi f_{c,i} t + \theta_{c,i})} e_{c,i} \quad (5)$$

where V_π is the half-wave voltage and φ_b is the DC bias phase. For OOK NRZ, $V(t)$ is expressed as

$$V(t) = \sum_n v_n \Pi\left(\frac{t - nT_b}{T_b}\right), \quad v_n = \begin{cases} V_{ON}, & a_n = 1 \\ V_{OFF} & a_n = 0 \end{cases} \quad (6)$$

So that cos(•) is close to 1 for the ON state and close to 0 for the OFF state.

As we used six channels, three channels are sent on H polarization and three channels on V polarization, a polarization combiner is used to combine all channels together and accordingly, the transmitted signal is expressed as

$$E_{Tx}(t) = \sum_{i=1}^{6} E_{MZM,i}(t) \quad (7)$$

The signal is then amplified with optical amplifier before propagating in the IsOWC channel.

4.2 IsOWC channel

The signal during propagation in IsOWC channel is affected by many factors like IS link, pointing errors, and losses. The signal after propagation in the IsOWC channel is then received with received optical power, P_{Rx}, which is given as:

$$P_{Rx} = P_{Tx} G_{Tx} G_{Rx} L_{Tx} L_{Rx} \eta_{Tx} \eta_{Rx} \left(\lambda / 4\pi L\right)^2 \quad (8)$$

where the symbols given in Eq. (8) with their notifications are given in Table 3.

Table 3 Symbols and notifications that given in Eq. (8)

Symbol	Notification and expression
P_{Tx}	Transmitted power.
G_{Tx}	Transmitter gain and is expressed as $\left(\pi D_{Tx}/\lambda\right)^2$, where D_{Tx} represents the diameter of transmitter lens.
G_{Rx}	Receiver gain and is expressed as $\left(\pi D_{Rx}/\lambda\right)^2$, where D_{Rx} represents the receiver lens diameter.
L_{Tx}	Transmitter loss factor and is given as $\exp(-G_{Tx}\theta_{Tx}^2)$, where θ_{Tx} denotes the angle of the transmitter pointing error.
L_{Rx}	Receiver loss factor and is given as $\exp(-G_{Rx}\theta_{Rx}^2)$, where θ_{Rx} denotes the receiver pointing error angle.
η_{Tx} and η_{Rx}	Transmitter and receiver optical efficiencies, respectively.
L	Propagation range.

4.3 Receiver

The incoming optical signal is first directed to a polarization beam splitter, which separates it into two parallel paths corresponding to the H and V polarization states. Each of these branches is then further divided into three optical channels. For every branch, data recovery is accomplished through a single photodiode detection (SPD) scheme, designed to retrieve the transmitted information. The SPD configuration integrates both a decoder and a subtractive decoder (S-Decoder), as illustrated in Fig. 2. The decoder structure mirrors the spectral characteristics of the transmitter's encoder. For instance, the decoder assigned to channel 1 employs four fiber Bragg gratings (FBGs) tuned at 850 nm, 835.2 nm, 855.6 nm, and 856.6 nm, whereas its S-Decoder counterpart uses a single FBG centered at 855.6 nm. This detection strategy effectively suppresses multiple access interference (MAI), a byproduct of the unity cross-correlation inherent to DPS codes. The S-Decoder output is subtracted from the main decoder output, and the difference signal is then fed into a photodetector (PD) for optical-to-electrical conversion. The resultant signal from the PD has a current, I, that expressed as [20]:

$$I = \frac{R\, P_{Rx}(w-1)}{C} \tag{9}$$

Where R denotes the PD responsivity, I_d refers to the dark current, w and C denote the code weight and code length respectively.

Finally, a low-pass filter (LPF) is applied to remove high-frequency noise, while a BER analyzer is used to evaluate performance and generate eye diagrams.

BER based on Gaussian approximation is expressed as [20]:

$$BER = \sqrt{\frac{SNR}{8}} \quad (10)$$

The SNR is given as [20]:

$$SNR = \frac{(I)^2}{o_{shot}^2 + o_{Thermal}^2} = \frac{\left(\frac{R\,P_{Rx}(w-1)}{C}\right)^2}{2eB_e\left(\frac{R\,P_{Rx}(w-1)}{C} + I_d\right) + \frac{4k_BT_aB_e}{R_l}} \quad (11)$$

where e, B_e, I_d, k_B, T_a, and R_l are electron charge, electrical bandwidth, dark current, Boltzmann constant, absolute temperature, and receiver load resistance, respectively.

Based on Gaussian noise approximation, the corresponding BER is related to Q-factor by:

$$BER = \frac{1}{2}\,erfc\left(\frac{Q}{2}\right) \quad (12)$$

where $erfc$ is the complementary error function. This analytical relationship provides an accurate estimation of BER for optical communication systems under thermal and shot noise conditions. In the current study, the Q-factor is evaluated from simulated eye diagrams and power levels, following this relation, to validate system performance under different transmitter powers, propagation ranges, pointing errors, aperture diameters, and optical efficiencies. It is calculated as the difference between the mean signal levels for receiving a bit '1' and a bit '0', divided by the sum of their standard deviations as follows:

$$Q = \frac{\mu_1 - \mu_0}{\sigma_1 + \sigma_0} \quad (13)$$

where μ_1 and μ_0 are the mean signal values for the '1' and '0' bits, respectively, and σ_1 and σ_0 are their corresponding standard deviations.

5. Results and Discussion

The proposed system is simulated with optisystem ver. 21 with components based on the above-mentioned equations have parameters values given in Table 4 [12, 14, 15, 19].

Table 4 Parameters values for proposed system

Parameter	Value
Transmitter	
PRBSG sequence length	1024
R_b	20 Gbps per channel
Line coding modulation	NRZ
Amplifier gain	10 dB
Number of channels	6
Ωw	3
C	12
MZM extinction ratio	30 dB
IsOWC channel	
P_{Tx}	27 - 30 dBm
λ	850 nm
D_{Tx}	15 cm
η_{Tx}	0.7, 0.8, and 0.9
θ_{Tx}	1 - 1.5 μrad
L	12,000, 14,000, and 16,000 km
D_{Rx}	10 -20 cm
η_{Rx}	0.7, 0.8, and 0.9
θ_{Rx}	1 - 1.5 μrad
Receiver	
R	0.8 A/W
Receiver Sensitivity	-21 dBm
I_d	5 nA
B_e	$0.75\times R_b$
T_a	290 K
R_l	50

The results are presented in four parts, addressing the optimization of transmit power, pointing error, receiver aperture diameter, and optical efficiency for the proposed IsOWC system using 2D DPS codes.

5.1 Optimization of Transmit Power

In this work, data transmission is considered between two intersatellites separated by distances of 12,000 km, 14,000 km, and 16,000 km. The BER and Q-factor performances under varying transmit power levels are analyzed, with the results shown in Fig. 3. For clarity, only the results of channel 1 are presented, as it demonstrates the lowest performance. It is observed that increasing the transmit power improves both BER and Q-factor. Additionally, the link distance has a significant impact: as shown in Fig. 3(b), extending the range from 12,000 km to 16,000 km increases log(BER) from –22.53 to –8.22, while Fig. 3(a) illustrates that the Q-factor decreases from 9.86 to 5.69 over the same distance range. Since the threshold log(BER) is –2.42, and the proposed system achieves values below this threshold for all transmit powers between 27 dBm and 30 dBm,

reliable communication is ensured. Accordingly, the system supports a total capacity of 20 Gbps × 6 channels = 120 Gbps.

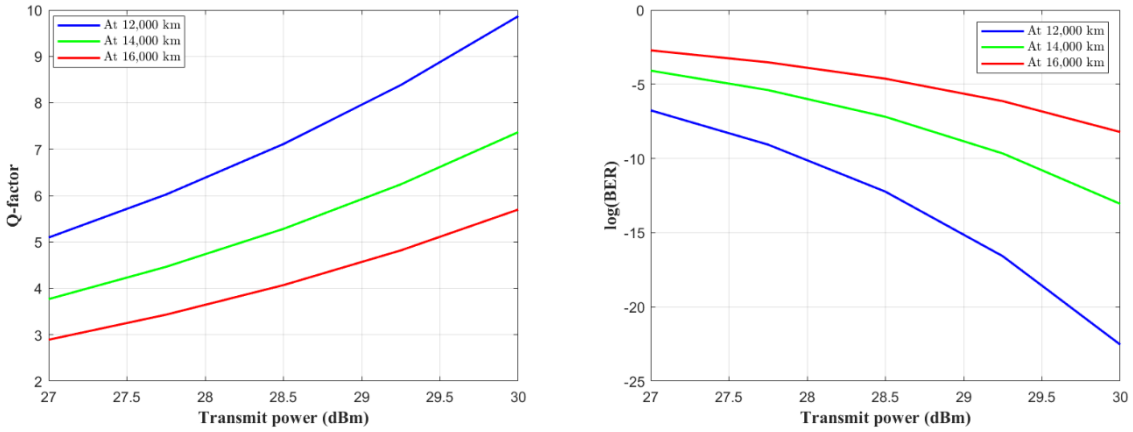

(a) (b)

Figure 3 Performance of proposed IsOWC based on 2D DPS code at varying transmit power and ranges: (a) Q-factor and (b) BER.

The eye diagram is a visual metric used to assess the quality of the received signal. Figure 4 (a) – (c) illustrates the eye diagrams for channel 2 at a transmit power of 30 dBm over ISL distances of 12,000 km, 14,000 km, and 16,000 km respectively. The large eye openings observed in all cases indicate that the transmitted signals are received with high quality. Although the eye opening slightly decreases as the distance increases, it remains sufficiently wide to ensure reliable detection and error-free performance.

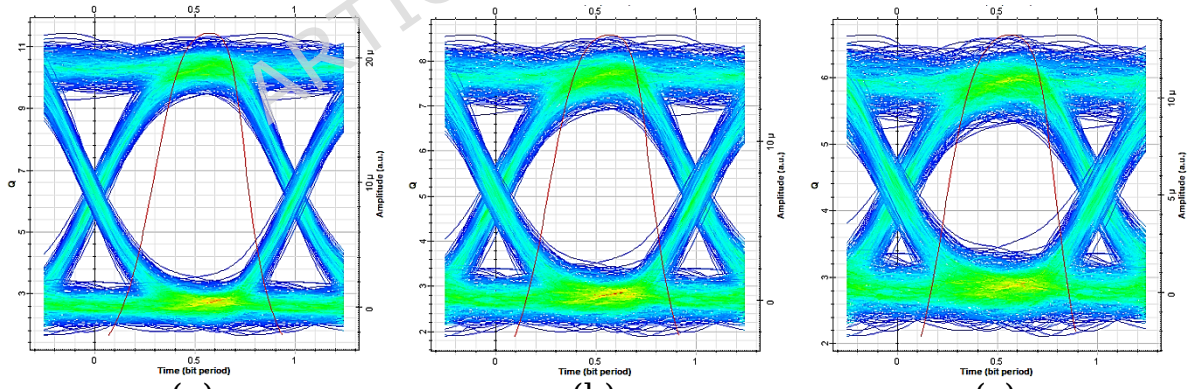

(a) (b) (c)

Figure 4 Eye diagrams for proposed system at 30 dBm transmit power and ranges of (a) 12,000 km, (b) 14,000 km, and (c) 16,000 km.

5.2 Impact of Receiver Pointing Error on System Performance

Pointing errors are a critical impairment in IsOWC systems due to the extremely narrow beam divergence of optical carriers. Even slight misalignments between the transmitter and receiver caused by satellite vibrations, tracking inaccuracies, or thermal distortions can lead to

significant power loss at the receiver aperture. This degradation directly impacts key performance metrics such as BER and Q-factor, making the evaluation of pointing error effects essential for reliable system design. In this section, the performance degradation caused by receiver-side pointing errors is analyzed, as such errors dominate in practical inter-satellite optical links due to vibration of the receiver's optical payload and tracking inaccuracy. The transmitter terminal is assumed to have negligible misalignment owing to its stable optical platform and fine-pointing control.

In this study, we investigate the impact of receiver pointing errors at different propagation ranges in space on the proposed IsOWC system employing 2D DPS codes, with the results illustrated in Fig. 5. It can be observed that increasing the pointing error angle leads to a noticeable degradation in system performance. For instance, the Q-factor decreases from 6.45 to 3.04 as the pointing error angle increases from 1 μrad to 1.5 μrad. Similarly, the log(BER) deteriorates from -10.27 to -6.98 over the same range of pointing error angles. Moreover, the transmission distance between satellites significantly influences the effect of pointing errors. The impact is less severe at shorter distances compared to longer ones. For example, at 12,000 km, the Q-factor and log(BER) values are 5.35 and -7.37, respectively, for a receiver pointing error of 1.5 μrad. However, at 14,000 km with the same receiver pointing error angle, the corresponding values degrade further to 3.96 and -4.43.

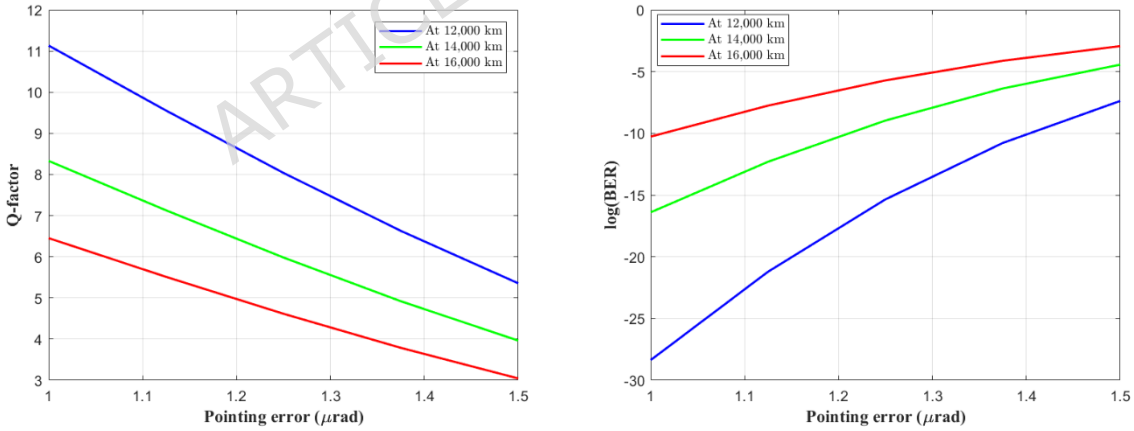

(a) (b)

Figure 5 Performance of proposed IsOWC based on 2D DPS code at varying receiver pointing error angles and ranges: (a) Q-factor and (b) BER.

Similarly, the eye diagrams at different propagation distances are presented for the proposed IsOWC system with a pointing error angle of 1.5 μrad are shown in Fig. 6. Although the eye opening becomes narrower as the ISL increases, the transmitted signals are still successfully received.

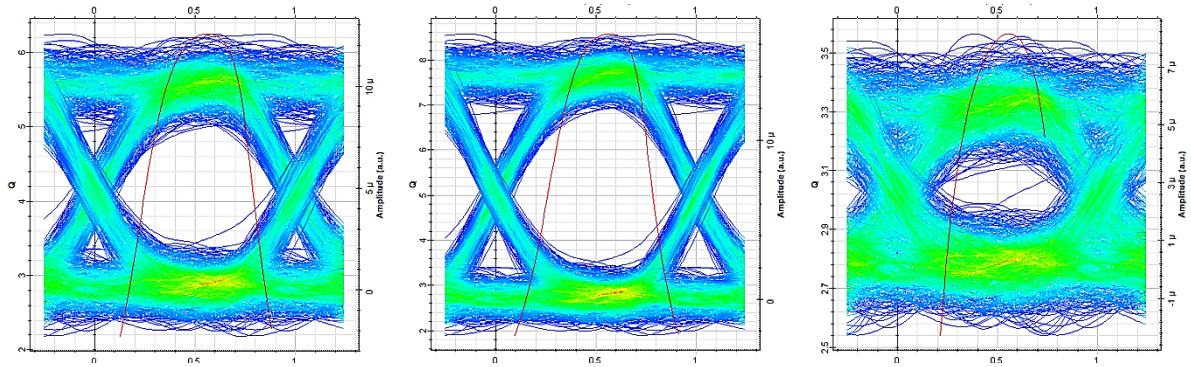

(a) (b) (c)

Figure 6 Eye diagrams for proposed system at 1.5 μrad receiver pointing error and ranges of (a) 12,000 km, (b) 14,000 km, and (c) 16,000 km.

5.3 Receiver Aperture Diameter

The receiver aperture diameter plays a critical role in IsOWC systems by determining the amount of collected optical power. Larger apertures improve signal reception and system performance, while smaller apertures increase power loss and degrade metrics such as BER and Q-factor. Fig. 7 illustrates the impact of receiver aperture diameter on the proposed IsOWC system. As the aperture increases from 10 cm to 20 cm, log(BER) improves significantly across all link distances, increasing from -7.83 to -37.53 at 12,000 km, from -4.69 to -21.67 at 14,000 km, and from -3.09 to -13.51 at 16,000 km. Correspondingly, the Q-factor, shown in Fig. 7(a), rises from 5.54 dB to 12.88 dB at 12,000 km, from 4.10 dB to 9.66 dB at 14,000 km, and from 3.15 dB to 7.50 dB at 16,000 km. These indicate that larger apertures collect more optical power, reduce path loss, and enhance signal quality, resulting in improved BER and Q-factor performance, with shorter links benefiting more strongly from aperture enlargement.

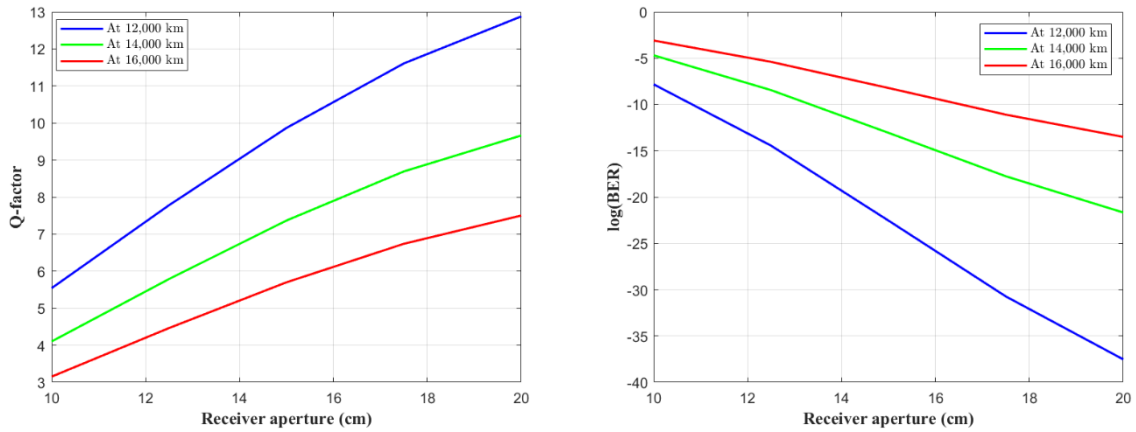

(a) (b)

Figure 7 Performance of proposed IsOWC based on 2D DPS code at different receiver aperture diameters and ranges: (a) Q-factor and (b) BER.

The eye diagrams of the proposed IsOWC system, with a receiver aperture of 20 cm, are depicted for ISL distances of 12,000 km, 14,000 km, and 16,000 km in Fig. 8. As the propagation distance increases, a slight reduction in eye opening is observed, reflecting the increased path loss and signal attenuation over longer links. Nevertheless, the eye remains sufficiently open across all distances, indicating that the transmitted signals are received with high fidelity and that the system maintains robust performance even at extended separations.

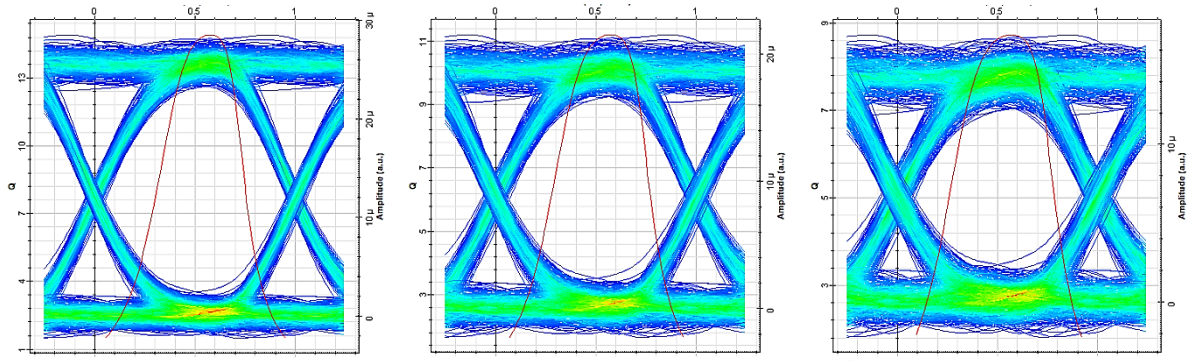

(a) (b) (c)

Figure 8 Eye diagrams for proposed system at 20 cm receiver aperture diameter and ranges of (a) 12,000 km, (b) 14,000 km, and (c) 16,000 km.

5.4 Role of Optical Efficiency in System Performance

Optical efficiency determines the fraction of transmitted power successfully received and converted to an electrical signal in IsOWC systems. Higher efficiency improves BER and Q-factor, making its evaluation essential for assessing system performance.

Figure 9 demonstrates the impact of optical efficiency on the performance of the proposed IsOWC system across different ISL distances. As shown in Fig. 9(a), increasing the optical efficiency from 0.7 to 0.9 significantly improves the Q-factor for all ranges; for instance, at 10,000 km, the Q-factor rises from 8.66 dB to 13.84 dB, while at 16,000 km it increases from 3.49 dB to 5.70 dB. Correspondingly, Fig. 9(b) shows that higher optical efficiency drastically reduces the log(BER), enhancing signal reliability. At 10,000 km, log(BER) decreases from -17.64 for an efficiency of 0.7 to -43.16 for 0.9, whereas at 16,000 km, it improves from -3.61 to -8.22. These results indicate that increasing optical efficiency mitigates the effects of path loss and signal attenuation, thereby improving both BER and Q-factor.

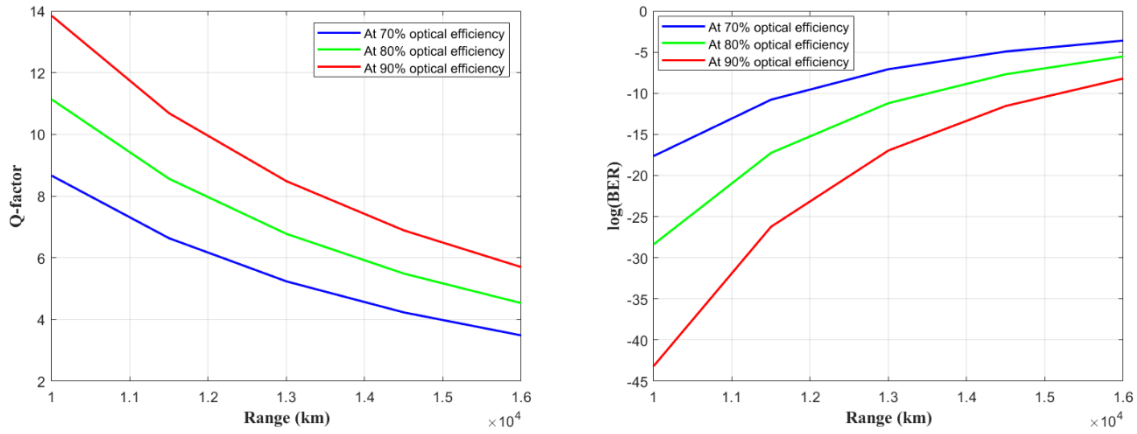

(a) (b)

Figure 9 Performance of proposed IsOWC based on 2D DPS code at various ISL ranges and different optical efficiencies: (a) Q-factor and (b) BER.

Finally, eye diagrams at 70%, 80%, and 90% for the proposed systems at ISL of 16,000 km are displayed in Fig. 10. One can observe that eye opening at optical efficiency of 90% is larger than those at 80% and 70%.

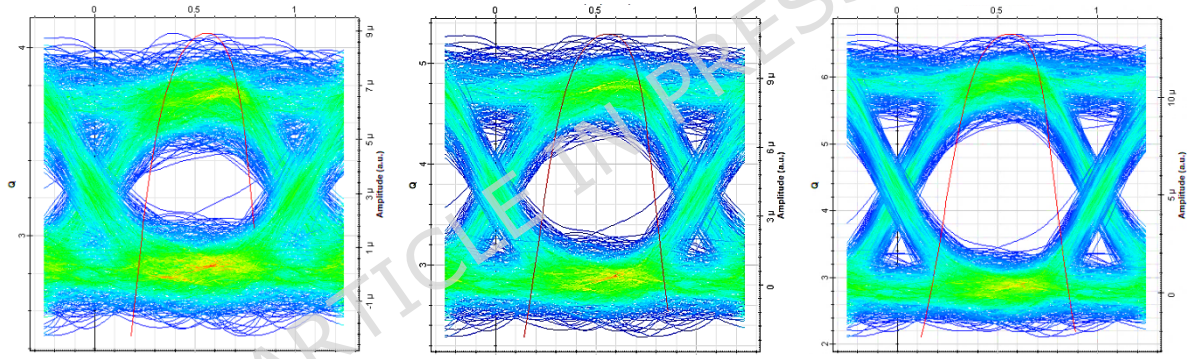

(a) (b) (c)

Figure 10 Eye diagrams for proposed system at 16,000 km and optical efficiencies of (a) 70% (b) 80%, and (c) 90% km.

6. Conclusion

In this paper, we investigated the performance of the proposed IsOWC system employing 2D DPS code under various practical conditions. The study analyzed the influence of propagation distance, receiver aperture diameter, and optical efficiency on performance metrics, including Q-factor, BER, and eye diagram. The results confirm that while performance degrades with longer inter-satellite distances, significant improvements can be obtained by increasing the receiver aperture diameter and optical efficiency. For instance, doubling the aperture diameter from 10 cm to 20 cm, or improving optical efficiency from 0.7 to 0.9, produced a clear enhancement in link performance. Eye diagram evaluations further revealed that, although the eye opening narrowed at longer transmission distances, the signals could still be reliably reconstructed, thereby

validating the feasibility of the system for long-haul ISLs. The use of 2D OCDMA in ISOWC system ensures secure data transmission since only receivers equipped with the correct decoding sequence can successfully detect the signal. This inherent security feature led to recommending the implementation of our proposed IsOWC system in sensitive applications such as defense and strategic satellite communications. Additionally, the overall transmission capacity of 120 Gbps that achieved by our proposed system, positioning it as a highly competitive solution for next-generation satellite networks as high-speed inter-satellite backbone links, Earth observation satellite networks, and deep-space exploration missions.

As for future work, we suggest broadening this study to consider additional real-world impairments, including satellite-induced jitter, and atmospheric turbulence within hybrid Earth-to-satellite communication scenarios. We also plan to investigate the integration of advanced error-control coding, adaptive optics, and artificial intelligence (AI) based optimization techniques to further enhance system robustness. Hardware implementation and experimental validation are also planned to demonstrate the practical viability of the proposed system in operational inter-satellite networks.

Data Availability Statement: The data and material generated during this study will be available from the corresponding author on request.

Funding: This work was funded by the Deanship of Graduate Studies and Scientific Research at Jouf University under grant No. (DGSSR-2025-FC-01040)

References

1. Hu, J. H., Yeung, L. K. & Li, T. Routing and re-routing in a LEO/MEO two-tier mobile satellite communications system with inter-satellite links. *Proc. IEEE Int. Conf. Commun.*, New Orleans, Louisiana, USA, 134–138 (2000).
2. Aguiar-Castillo, L., Guerra, V., Rufo, J., Rabadan, J. & Perez-Jimenez, R. Survey on optical wireless communications-based services applied to the tourism industry: potentials and challenges. *Sensors* 21, 6282 (2021). https://doi.org/10.3390/s21186282
3. Tawfik, M. M., Sree, M. F. A., Abaza, M. & Ghouz, H. H. M. Performance analysis and evaluation of inter-satellite optical wireless communication system (IsOWC) from GEO to LEO at range 45,000 km. *IEEE Photonics J.* 13, 1–6 (2021). https://doi.org/10.1109/jphot.2021.3104819

4. Sotom, M., Benazet, B., Le Kernec, A. & Maignan, M. Microwave photonic technologies for flexible satellite telecom payloads. In Proc. 35th European Conf. on Optical Communications (ECOC 2009), Vienna, Austria, 20–24 September 2009.
5. Heine, F., Kämpfner, H., Czichy, R., Meyer, M. & Lutzer, M. Optical inter-satellite communication operational. In Proc. MILCOM Military Communications Conf., Baltimore, MD, USA, 1583–1587 (2010). https://doi.org/10.1109/milcom.2010.5680175
6. Singh, M. & Malhotra, J. Modeling and performance analysis of 400 Gbps CO-OFDM based inter-satellite optical wireless communication (IsOWC) system incorporating polarization division multiplexing with enhanced detection. Wireless Pers. Commun. 111, 495–511 (2020). https://doi.org/10.1007/s11277-019-06870-5
7. Patnaik, P. S. B. Inter-satellite optical wireless communication system design and simulation. IET Commun. 6, 2561–2567 (2012).
8. Benzi, T. D. E., Shurmer, M. J. I., Lutzer, M. & Kuhlmann, S. Optical inter-satellite communication: the alphasat and sentinel-1A in-orbit experience. In Proc. 14th Int. Conf. Space Operations, Daejeon, Korea, 1–13 (2016).
9. Japan Aerospace Exploration Agency. Successful achievement of the world's fastest optical inter-satellite communication at a speed of 1.8 Gbps between the Laser Utilizing Communication System (LUCAS) and the Advanced Land Observing Satellite-4 "DAICHI-4". Press release, 8 October 2024. Available at: https://global.jaxa.jp/press/2024/10/20241008-1_e.html (Accessed: 25 August 2025).
10. Kaur, R. & Kaur, H. Comparative analysis of chirped, AMI and DPSK modulation techniques in IS-OWC system. Optik 154, 755–762 (2018). https://doi.org/10.1016/j.ijleo.2017.10.108
11. Abdulwahid, M. M. & Kurnaz, S. The channel WDM system incorporates of optical wireless communication (OWC) hybrid MDM-PDM for higher capacity (LEO-GEO) inter satellite link. Optik 273, 170449 (2023). https://doi.org/10.1016/j.ijleo.2022.170449
12. Armghan, A., Alsharari, M., Aliqab, K., Singh, M., Aly, M. H. & Abd El-Mottaleb, S. A. A 4 × 20 Gbps inter-satellite optical wireless communication system based on orbital angular momentum multiplexing: performance evaluation. Opt. Quantum Electron. 56, 9 (2024). https://doi.org/10.1007/s11082-024-07338-y
13. Kumar, S., Gill, S. S. & Singh, K. Performance investigation of inter-satellite optical wireless communication (IsOWC) system employing multiplexing techniques. Wireless Pers. Commun. 98, 1461–1472 (2017). https://doi.org/10.1007/s11277-017-4926-4

14. Grover, A. & Sheetal, A. A 2 × 40 Gbps mode division multiplexing based inter-satellite optical wireless communication (IsOWC) system. Wireless Pers. Commun. 114, 2449–2460 (2020). https://doi.org/10.1007/s11277-020-07483-z
15. Sharma, V. & Kumar, N. Modeling of 2.5 Gbps-intersatellite link (ISL) in inter-satellite optical wireless communication (IsOWC) system. Optik 124, 6182–6185 (2013). https://doi.org/10.1016/j.ijleo.2013.04.094
16. Chaudhary, S., Kapoor, R. & Sharma, A. Empirical evaluation of 4 QAM and 4 PSK in OFDM-based inter-satellite communication system. J. Opt. Commun. 40, 143–147 (2019). https://doi.org/10.1515/joc-2017-0059
17. Zhu, Y., Xu, G., Gao, M., Chu, H. & Song, Z. Average bit-error rate analysis of an inter-satellite optical communication system under the effect of perturbations. Opt. Express 32, 36796–36810 (2024).
18. Xu, G., Yin, L., Zhu, Y., Wang, H. & Song, H. Satellite-to-ground optical communication systems under orbital deviations and atmospheric turbulence: channel modeling and performance analysis. Opt. Express 33, 18912–18927 (2025).
19. Singh, M. et al. A high-speed integrated OFDM/DPS-OCDMA-based FSO transmission system: impact of atmospheric conditions. Alexandria Eng. J. 77, 15–29 (2023). https://doi.org/10.1016/j.aej.2023.06.077.
20. Abd El-Mottaleb, S. A., Métwalli, A., ElDallal, T. A., Hassib, M., Fayed, H. A. & Aly, M. H. Performance evaluation of PDM/SAC-OCDMA-FSO communication system using DPS code under fog, dust and rain. Opt. Quant. Electron. 54, 750 (2022).